Implicit Radiation & Chemical Ionization FLD Solver in Enzo

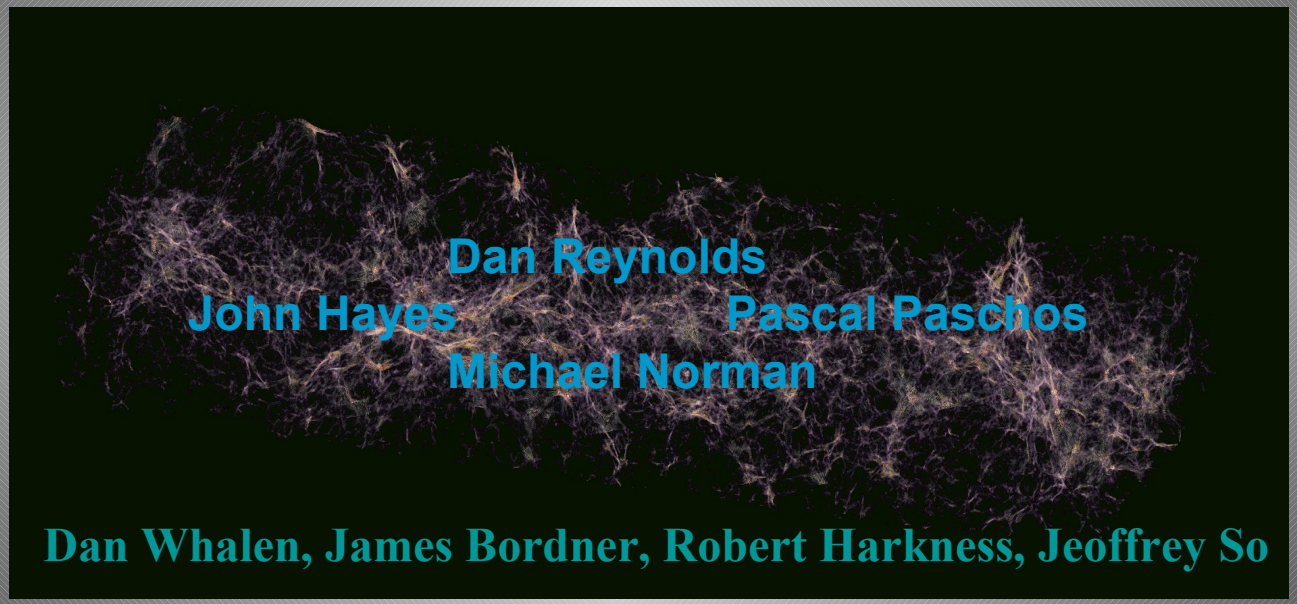

- *Numerical Method*
- *Tests*
  - *Streaming radiation tests*
  - *Static isothermal monochromatic*
  - *Static blackbody*
  - *Test5 – Classical HII expansion*
  - *Cosmological I-fronts*
- *Solver Scalability*

Some standard Enzo benchmarks

- *ISM turbulence (no DM)*
  - *production: 2048^3 (UG) on 4096 cores*
  - *capability: 4096^3 (UG) on 16,000 cores*
- *Cosmology*
  - *production (UG) e.g. LAF: 2048^3 (mesh) + 2048^3 (DM particles)*
    - *2048 cores*
  - *capability (UG): 2944^3 (mesh) + 2944^3 (DM particles)*
    - *12167 cores*
  - *production (AMR): L7 - 1024^3 (mesh) + 1024^3 (DM particles) [root grid] (L7: 7 levels of refinement)*
    - *400,000 subgrids at z=5.8*
    - *2048 cores*

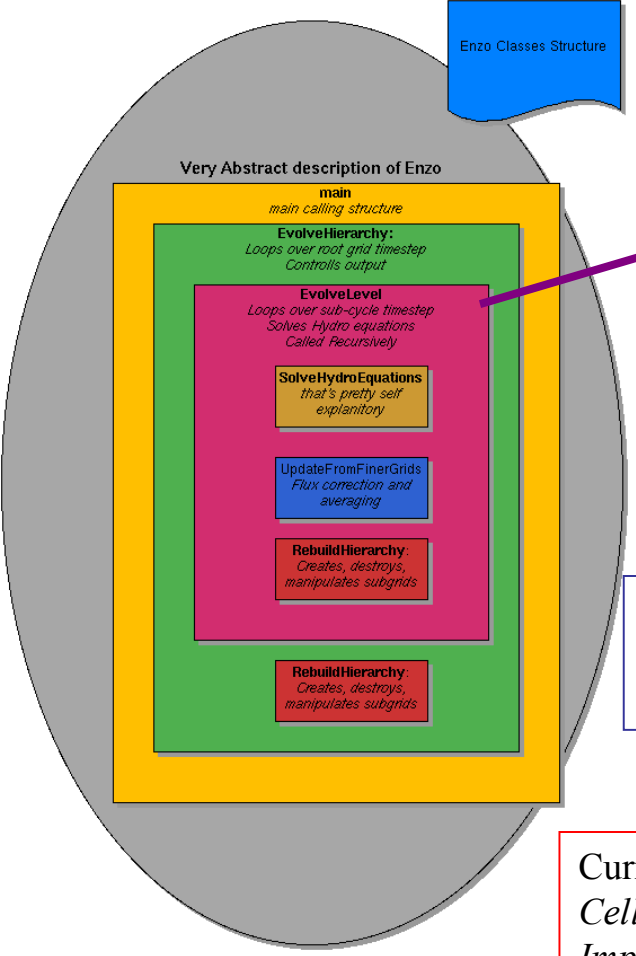

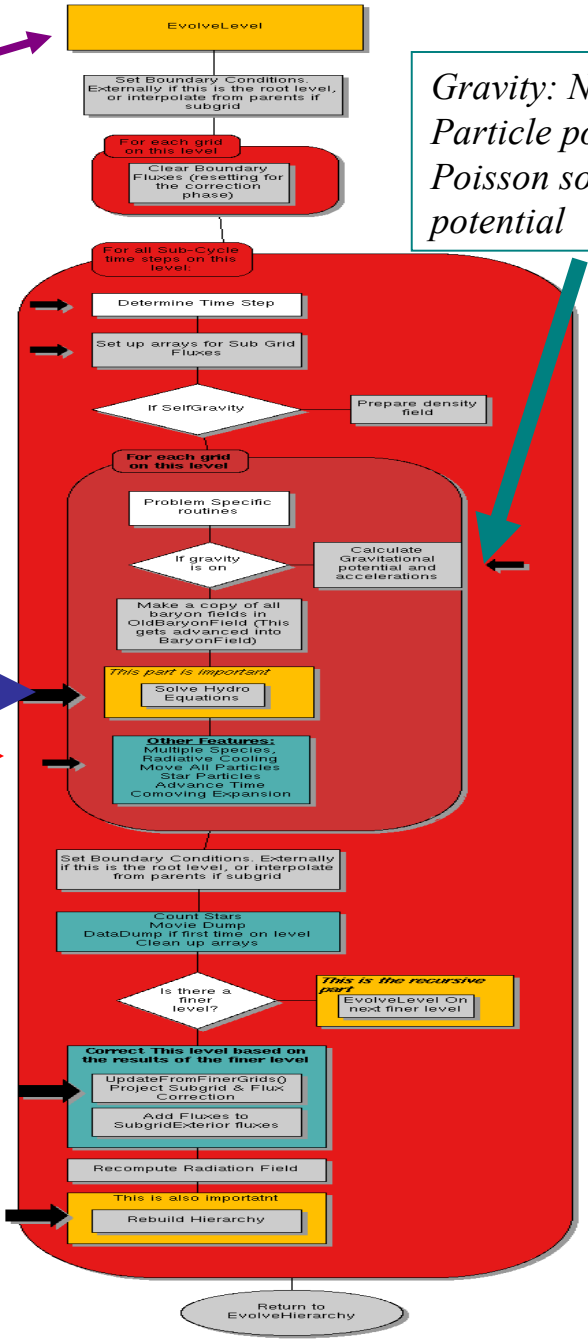

Gravity: N-body for Particle position then Poisson solve for grav potential

Hydro: Eulerian PPM explicit coupled to chemistry through gas energy

Current species ionization module
Cell-local, uniform UVB driven, Implicit chemistry + explicit gas energy

RT species ionization module
*Cell-non-local, J(**x**,v,t) driven, implicit chemistry/gas energy/ J(**x**,v,t)*

Enzo Numerics

The PDE system is solved with a method of lines approach using:

- Finite volume spatial approximation, with PPM flux reconstruction.
- Explicit time integration for the hydrodynamic quantities ρ_b, $\mathbf{v}_b$ and e,
- Operator-split coupling to a steady-state Poisson solve for the gravitational potential ϕ, based on
  - an FFT-based solve for periodic domains, or
  - a geometric multigrid solve for isolated/mixed BC domains.
- Block-structured AMR discretization of Ω, with inter-level couplings via
  - flux/refluxing to ensure conservation across levels,
  - time subcycling of refined grids for CFL stability.

Goals

I. Extend Enzo code for cosmological hydrodynamics + gravity to include radiation transport & chemical ionization, enabling:

   - studies of self-regulated star formation,
   - predictions on the epoch of cosmic reionization, and
   - predictions on the observed properties of early galaxies.

II. Accurately model stiff cosmological radiation transfer and chemical ionization kinetics processes.

III. Incorporate new solver in Enzo code so that coupling respects hydrodynamics approach (shocks), but tightly couples physical processes.

IV. Enable very-large-scale simulations ($\mathcal{O}(10^6)$ processors).

Flux-Limited Diffusion Radiation Transfer

We approximate the radiative flux as a function of the energy density gradient,

$$\mathbf{F}_\nu = -\frac{1}{a} D \nabla E_\nu ,$$

where $D : \Omega \rightarrow I\!R^{3\times 3}$ is the *flux limiter*, $D = D(E_\nu, \nabla E_\nu)$.

With this approximation, the radiation energy equation becomes

$$\partial_t E_\nu + \tfrac{1}{a}\nabla \cdot (E_\nu \mathbf{v}_b) - \tfrac{1}{a^2}\nabla \cdot (D \nabla E_\nu) - \tfrac{1}{ca^3} (\nabla (D \nabla E_\nu)) : (\nabla \mathbf{v}_b)$$
$$= \nu \tfrac{\dot{a}}{a} \partial_\nu E_\nu - 3\tfrac{\dot{a}}{a} E_\nu + 4\pi\eta_\nu - ck_\nu E_\nu .$$

Notes:

- The emissivity $\eta_\nu : \Omega \rightarrow I\!R$ may depend on the energy e, and abundances $\mathbf{n}_i$.
- The opacity $k_\nu : \Omega \rightarrow I\!R$ depends on the chemical abundances $\mathbf{n}_i$.
- D allows a smooth transition between diffuse and free-streaming limits.

Coupled Matter-Radiation System

Combining the original, cosmological hydrodynamic system with the new chemical and radiation equations, we consider the coupled system,

$$
\begin{aligned}
\nabla^2\phi &= \frac{4\pi G}{a}\left(\rho_b + \rho_{dm} - \rho_0\right), \\
\partial_t\rho_b + \tfrac{1}{a}\mathbf{v}_b\cdot\nabla\rho_b &= -\tfrac{1}{a}\rho_b\nabla\cdot\mathbf{v}_b, \\
\partial_t\mathbf{v}_b + \tfrac{1}{a}\left(\mathbf{v}_b\cdot\nabla\right)\mathbf{v}_b &= -\tfrac{\dot{a}}{a}\mathbf{v}_b - \tfrac{1}{a\rho_b}\nabla p - \tfrac{1}{a}\nabla\phi, \\
\partial_t e + \frac{1}{a}\mathbf{v}_b\cdot\nabla e &= -\tfrac{2\dot{a}}{a}e - \tfrac{1}{a\rho_b}\nabla\cdot(p\mathbf{v}_b) - \tfrac{1}{a}\mathbf{v}_b\cdot\nabla\phi + G - \Lambda, \\
\partial_t\mathbf{n}_i + \nabla\cdot(\mathbf{n}_i\mathbf{v}_b) &= -3\tfrac{\dot{a}}{a}\mathbf{n}_i - \mathbf{n}_i\Gamma_i^{ph} + \alpha_{i,j}^{rec}\,\mathbf{n}_e\mathbf{n}_j, \\
\partial_t E + \tfrac{1}{a}\nabla\cdot(E\mathbf{v}_b) - \tfrac{1}{a^2}\nabla\cdot(D\nabla E) &= -4\tfrac{\dot{a}}{a}E + 4\pi\eta - ckE. \qquad \text{(Grey)}
\end{aligned}
$$

In the gas energy equation, $G = G(E,\mathbf{n}_i)$ and $\Lambda = \Lambda(E,\mathbf{n}_i)$ are the heating rate and cooling rates, corresponding to energy sources and sinks due to radiation and chemical couplings.

Formulation of Implicit Coupled System

We decompose the energy into two parts, $e = e_h + e_c$. e_h arises from the explicit hydrodynamic advection, e_c is the correction due to chemical-radiation coupling,

$$\partial_t(e_h + e_c) + \tfrac{1}{a}\mathbf{v}_b \cdot \nabla e = -\tfrac{2\dot{a}}{a}(e_h + e_c) - \tfrac{1}{a\rho_b}\nabla \cdot (p\mathbf{v}_b) - \tfrac{1}{a}\mathbf{v}_b \cdot \nabla\phi + G - \Lambda.$$

Since Enzo evolves ρ_b, $\mathbf{v}_b$ & e_h ~~and advects E & $\mathbf{n}_i$~~ explicitly, we solve the remainder implicitly to evolve $\mathbf{n}_i$, E and the energy correction e_c,

$$\begin{aligned}
\partial_t e_c &= -2\tfrac{\dot{a}}{a}e_c + G - \Lambda, \\
\partial_t \mathbf{n}_i &= -3\tfrac{\dot{a}}{a}\mathbf{n}_i - \mathbf{n}_i\Gamma_i^{ph} + \alpha_{i,j}^{rec}\mathbf{n}_e\mathbf{n}_j, \\
\partial_t E &= \tfrac{1}{a^2}\nabla \cdot (D\,\nabla E) - 4\tfrac{\dot{a}}{a}E + 4\pi\eta - ckE.
\end{aligned}$$

- Such splitting into separate advection and reaction-diffusion processes may limit the solver accuracy and stability.
- However, each process uses the best-suited algorithm, and induced errors are no greater than the original gravity/dark matter splitting.

Implicit Time Discretization

We consider a 2-level θ-scheme for implicit integration of the updated energy e_c^n, radiation energy density E^n and chemical species densities $\mathbf{n}_i^n$:

$$
\begin{aligned}
e_c^n + \Delta t \theta \mathcal{L}_e^n \left(e_c, \mathbf{n}_i, E\right) &= g_e^{n-1}, \\
\mathbf{n}_i^n + \Delta t \theta \mathcal{L}_{\mathbf{n}}^n \left(e_c, \mathbf{n}_i, E\right) &= g_{\mathbf{n}_i}^{n-1}, \\
E^n + \Delta t \theta \left[\mathcal{D}_E^n \left(E\right) + \mathcal{L}_E^n \left(e_c, \mathbf{n}_i, E\right)\right] &= g_E^{n-1},
\end{aligned}
$$

where we have defined the component operators as

$$
\begin{aligned}
\mathcal{L}_e \left(e_c, \mathbf{n}_i, E\right) &= 2\tfrac{\dot{a}}{a} e_c - G + \Lambda, \\
\mathcal{L}_{\mathbf{n}} \left(e_c, \mathbf{n}_i, E\right) &= 3\tfrac{\dot{a}}{a} \mathbf{n}_i + \mathbf{n}_i \Gamma_i^{ph} - \alpha_{i,j}^{rec} \mathbf{n}_e \mathbf{n}_j, \\
\mathcal{L}_E \left(e_c, \mathbf{n}_i, E\right) &= 4\tfrac{\dot{a}}{a} E - 4\pi\eta + ckE, \\
\mathcal{D}_E(E) &= -\tfrac{1}{a^2} \nabla \cdot \left(D \nabla E\right),
\end{aligned}
$$

and $g_*^{n-1} = \Delta t(\theta - 1)\left[\mathcal{L}_*^{n-1} + \mathcal{D}_*^{n-1}\right]$ provide data from the previous time step.

Note: $\theta = 1 \rightarrow$ Implicit Euler, $\theta = \frac{1}{2} \rightarrow$ Trapezoidal rule (CN).

Implicit Solution Approach

Denoting the vector of unknowns $U = (e_c, \mathbf{n}_i, E)^T$, we define the nonlinear residual function, $f(U)$, over the time step $t^{n-1} \rightarrow t^n$ as

$$f(U) = U + \Delta t \theta \begin{pmatrix} \mathcal{L}_e \\ \mathcal{L}_{\mathbf{n}} \\ \mathcal{D}_E + \mathcal{L}_E \end{pmatrix} - \begin{pmatrix} g_e^{n-1} \\ g_{\mathbf{n}}^{n-1} \\ g_E^{n-1} \end{pmatrix}.$$

To evolve the coupled implicit system, we must solve the nonlinear problem $f(U) = 0$ for the updated vector U^n.

To this end, we use a *globalized Inexact Newton's Method*, that iterates toward the solution U^n through a sequence of linearized solutions:

1. Given an initial iterate U_0, we seek U_* such that $f(U_*) = 0$.
2. Repeat for each k, until $\|f(U_{k+1})\| < \varepsilon \approx 0$:
   (a) Approximately solve the linear system $J(U_k)\, S_k = -f(U_k)$
   (b) Update the approximate solution: $U_{k+1} = U_k + \lambda_k S_k$

$\|J(U_k)S_k + f(U_k)\| < \delta_k = 10^{-6}\|f(U_k)\|$ *Classic Inexact Newton*

Globalized Inexact Newton Details

Specifically,

- $J(U)$ provides a local linear model of $f(U)$ around U, $J(U) \equiv \frac{\partial}{\partial U} f(U)$.
- $0 < \lambda_k \leq 1$ is the *line search* parameter, chosen to ensure stability and globalization of the Newton algorithm.
- $U_0 \approx U^{n-1}$ is an initial guess for the time-evolved solution $U(t^n)$.
- $\|\cdot\|$ is a weighted L-2 norm, chosen to balance the different physical components.

Efficiency of this algorithm relies on a fast and robust solver for the linear Newton systems; robustness depends on an accurate initial guess.

Given a robust and scalable linear solver, the Newton algorithm exhibits fast convergence that for many PDE systems is independent of spatial resolution.

[see Dembo et al., 1982; Dennis & Schnabel; Brown & Saad, 1990; Allgower et al., 1986; Weiser et al., 2005]

Linear Newton Systems

The matrices arising in the inexact Newton algorithm have the form

$$J(U) = I + \Delta t \theta \begin{bmatrix} J_{e,e} & J_{e,\mathbf{n}} & J_{e,E} \\ J_{\mathbf{n},e} & J_{\mathbf{n},\mathbf{n}} & J_{\mathbf{n},E} \\ J_{E,e} & J_{E,\mathbf{n}} & J_{E,E} \end{bmatrix}$$

where the matrix blocks contain the components

$$J_{e,e} = [\partial_e \mathcal{L}_e] \qquad J_{e,\mathbf{n}} = [\partial_{\mathbf{n}_1} \mathcal{L}_e, \partial_{\mathbf{n}_2} \mathcal{L}_e, \ldots] \qquad J_{e,E} = [\partial_E \mathcal{L}_e]$$

$$J_{\mathbf{n},e} = \begin{bmatrix} \partial_e \mathcal{L}_{\mathbf{n}_1} \\ \partial_e \mathcal{L}_{\mathbf{n}_2} \\ \vdots \end{bmatrix} \quad J_{\mathbf{n},\mathbf{n}} = \begin{bmatrix} \partial_{\mathbf{n}_1} \mathcal{L}_{\mathbf{n}_1} & \partial_{\mathbf{n}_2} \mathcal{L}_{\mathbf{n}_1} & \cdots \\ \partial_{\mathbf{n}_1} \mathcal{L}_{\mathbf{n}_2} & \partial_{\mathbf{n}_2} \mathcal{L}_{\mathbf{n}_2} & \cdots \\ \vdots & \vdots & \ddots \end{bmatrix} \quad J_{\mathbf{n},E} = \begin{bmatrix} \partial_E \mathcal{L}_{\mathbf{n}_1} \\ \partial_E \mathcal{L}_{\mathbf{n}_2} \\ \vdots \end{bmatrix}$$

$$J_{E,e} = [\partial_e \mathcal{L}_E] \qquad J_{E,\mathbf{n}} = [\partial_{\mathbf{n}_1} \mathcal{L}_E, \partial_{\mathbf{n}_2} \mathcal{L}_E, \ldots] \qquad J_{E,E} = [\partial_E (\mathcal{D}_E + \mathcal{L}_E)]$$

Note: All blocks are local except for $J_{E,E}$, which contains spatial couplings.

Linear System Structure

Though the Jacobian contains couplings within and between variables, it has a very desirable structure:

- all inter-variable couplings occur only locally in space,
- spatial couplings are limited to the block $J_{E,E}$, consisting of a second order reaction-diffusion operator.

We therefore consider the Jacobian system $Jx = b$ to have the structure

$$\begin{bmatrix} M & U \\ L & D \end{bmatrix} \begin{pmatrix} x_M \\ x_E \end{pmatrix} = \begin{pmatrix} b_M \\ b_E \end{pmatrix}$$

where

$$M = I + \Delta t\theta \begin{bmatrix} J_{e,e} & J_{e,\mathbf{n}} \\ J_{\mathbf{n},e} & J_{\mathbf{n},\mathbf{n}} \end{bmatrix}, \qquad U = \Delta t\theta \begin{bmatrix} J_{e,E} \\ J_{\mathbf{n},E} \end{bmatrix} \qquad x_M = \begin{pmatrix} x_e \\ x_{\mathbf{n}} \end{pmatrix}$$

$$L = \Delta t\theta \begin{bmatrix} J_{E,e} & J_{E,\mathbf{n}} \end{bmatrix}, \qquad D = I + \Delta t\theta \begin{bmatrix} J_{E,E} \end{bmatrix}$$

Schur-CG-MG Linear Solver

Since M^{-1} is simple to compute (block-diagonal), we use a Schur complement formulation to solve for x,

$$Mx_M + Ux_E = b_M \quad \Rightarrow \quad x_M = M^{-1}(b_M - Ux_E),$$

hence,

$$Lx_M + Dx_E = b_E \quad \Rightarrow \quad (D - LM^{-1}U)x_E = b_E - LM^{-1}b_M.$$

The linear solve therefore proceeds as

(i) Set $y_M = M^{-1}b_M$, $T = M^{-1}U$

(ii) Solve for x_E from $(D - LT)x_E = b_E - Ly_M$

(iii) Recover $x_M = y_M - Tx_E$

The step (i) uses efficient direct solves [LAPACK].
The step (ii) uses a multigrid-preconditioned CG method [HYPRE].
Nearly all of this approach extends directly to the multi-frequency case.

Adaptive Time Step

Implicit ionization/radiation stability expands time step restrictions to the CFL hydrodynamic stability limit. For temporal accuracy of the solution within the hydro step we implement adaptive time steps to help satisfy prescribed accuracy requirements. We define a weight vector for the expected magnitude of the solution component at cell i by:

$$\omega_{i,v} = \sqrt{|U_{i,v}^{n+1} U_{i,v}^{pred}|} + 10^{-3}$$ (Constant value for normalized quantities)

We then estimate a local accuracy of the current time step as (N #cells, Ns #species):

$$\varepsilon_{loc} = \left(\frac{1}{N(N_s+2)} \left\| \frac{U^{n+1} - U^{pred}}{\omega} \right\|_p^p \right)^{1/p}$$

Where we use standard p-norm including p=∞ for the test problems which reduces the formula – by definition – to searching for a maximum value. Currently we use $\boldsymbol{U_{i,u}^{pred} = U_{i,u}^{n}}$. With this estimate we set the new time step equal to:

$$\Delta t^{n+1} = \frac{\tau_{\text{tol}} \Delta t^n}{\varepsilon_{loc}}$$

Streaming Radiation

signal speed tests

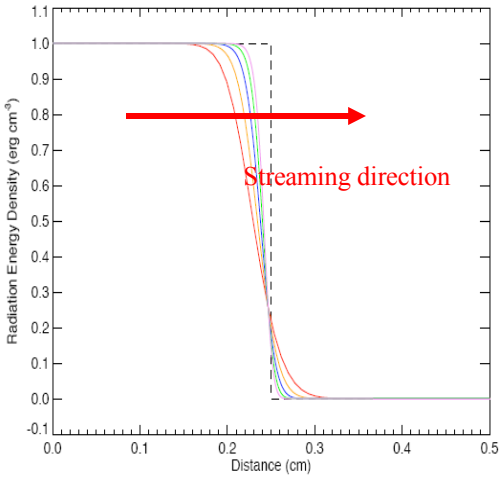

128^3 (red)
256^3 (orange)
512^3 (blue)
1024^3 (green)
2048^3 (violet)
Analytical (black)

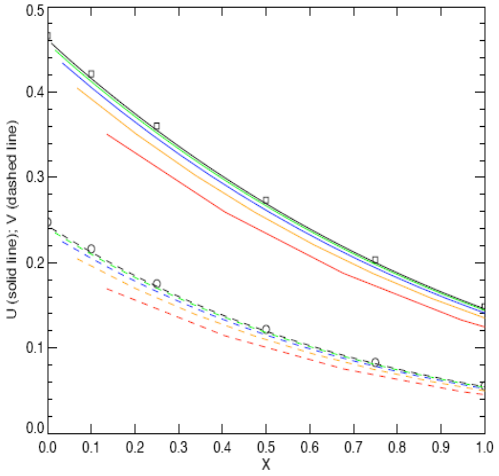

Non-equilibrium Marshak Waves (Pomraning 1979; Su & Olson 1996) test problem (points); mesh resolution convergence

$X \propto z$: dimensionless coordinate

$U \propto E(z,t)$

$V \propto T^4(z,t)$

normalized time = 1

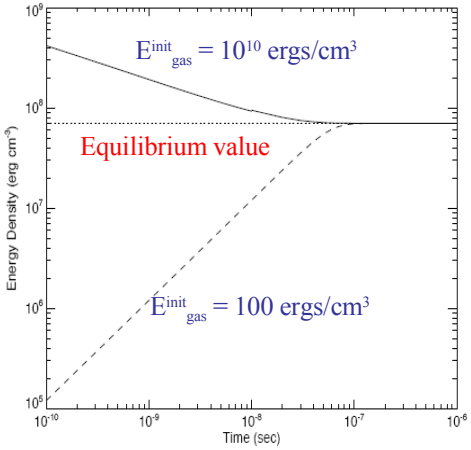

Turner & Stone (2001) test problem: Evolution to thermal equilibrium
$E_{rad} = 10^{12}$ ergs/cm^3

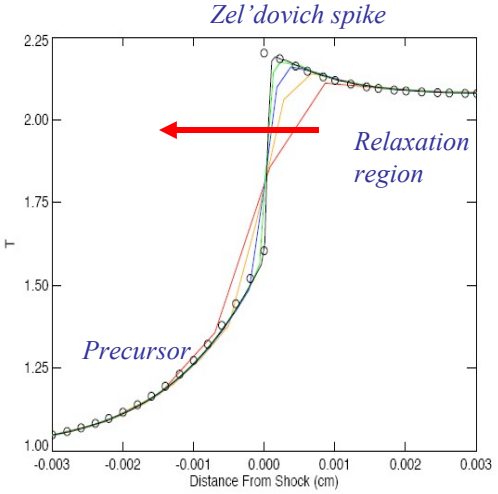

Radiating Shocks Lowrie & Edwards 2008) Planar, steady shock waves in the grey non-equilibrium diffusion limit, Mach-2 test problem (points) ; mesh resolution Convergence plot Temperature in pre-shock units

Test 1: Static isothermal HII Region (monochromatic)

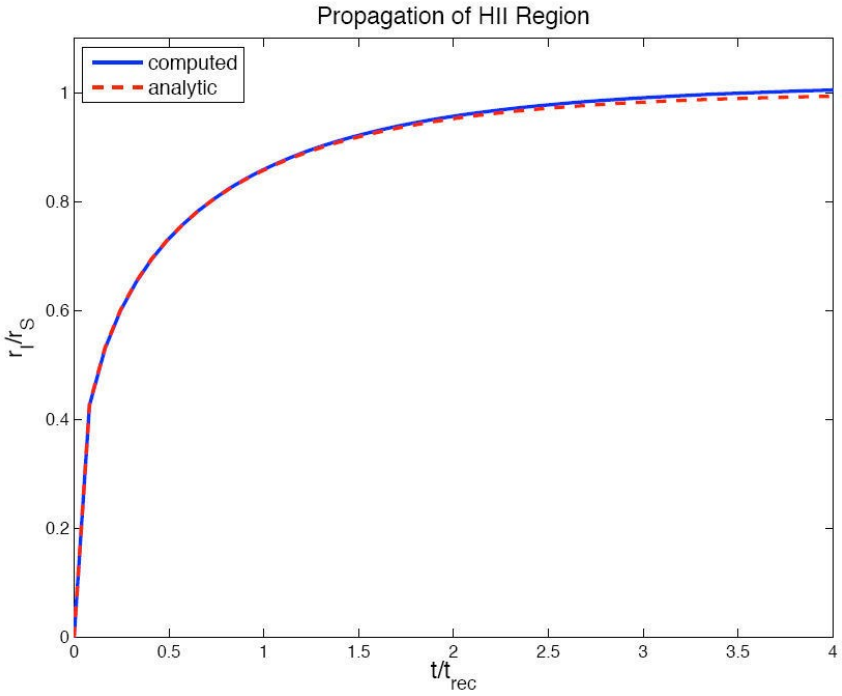

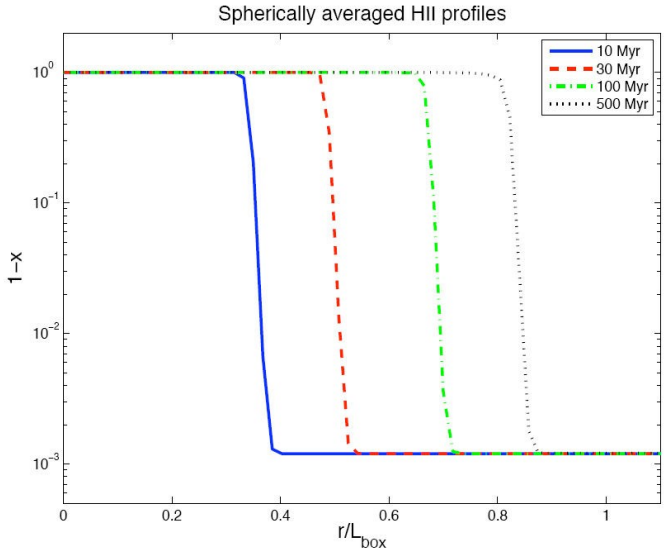

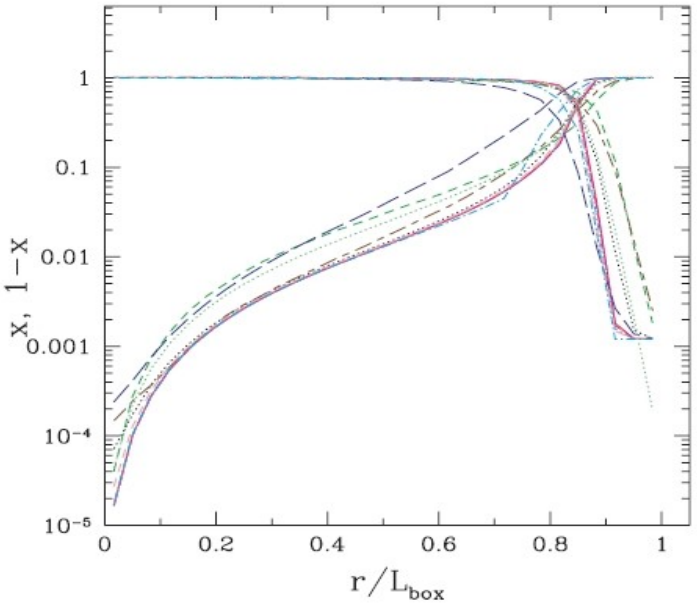

Test 2: Static HII Region (blackbody spectrum) HI,HII profiles

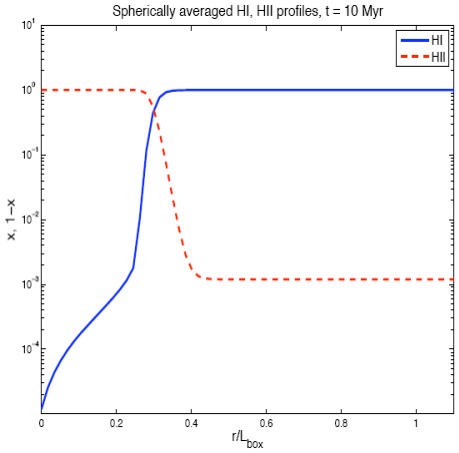

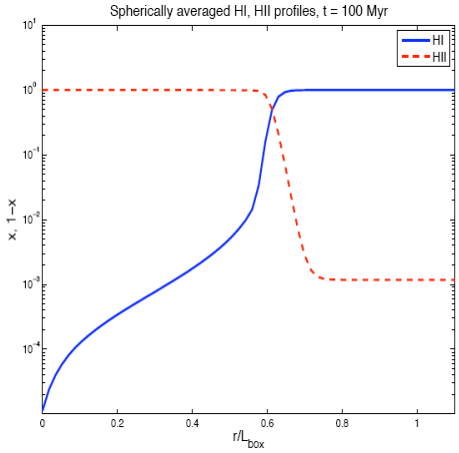

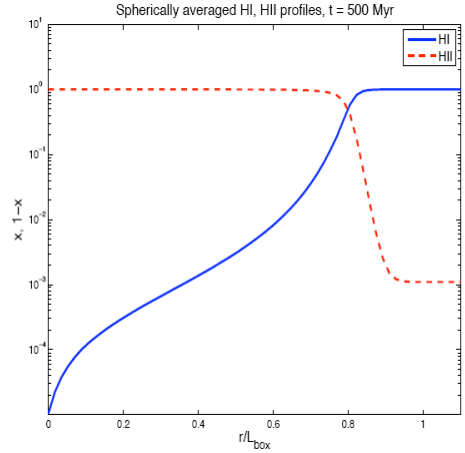

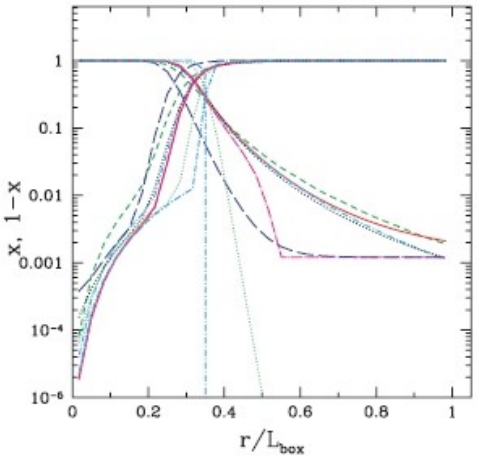

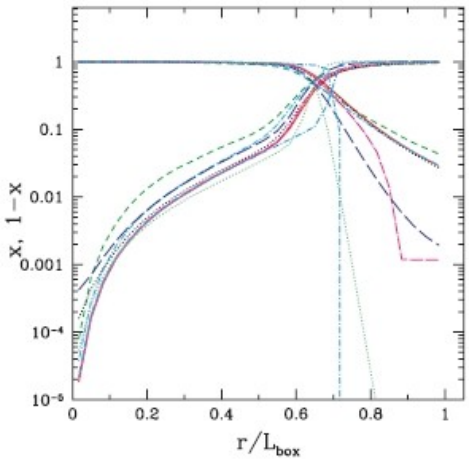

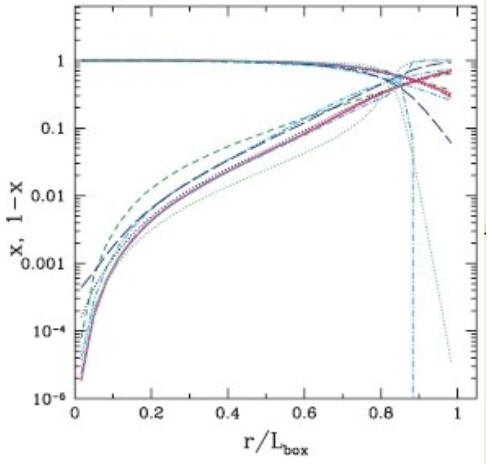

Test 2: Static HII Region (blackbody spectrum)

Temperature profiles

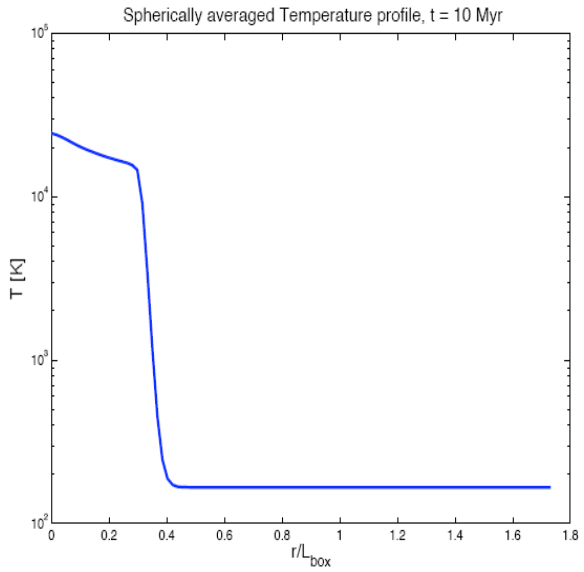

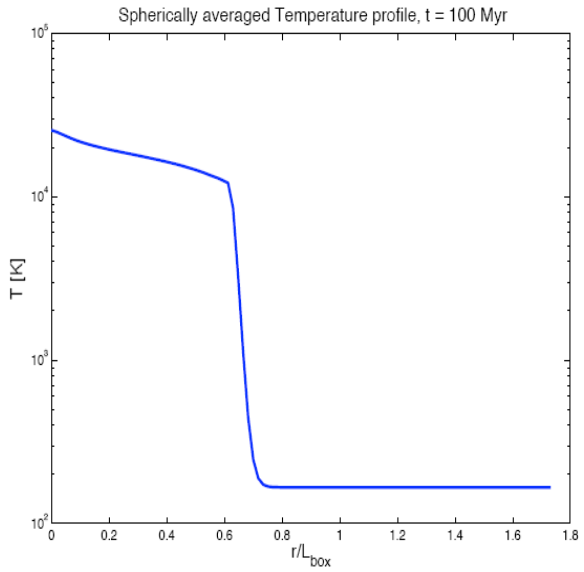

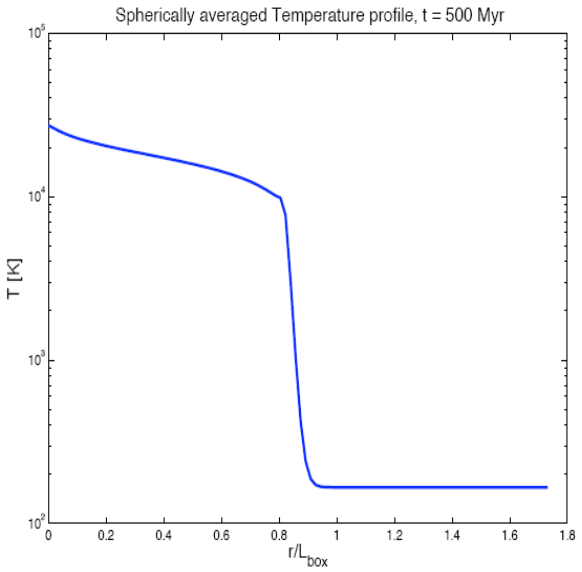

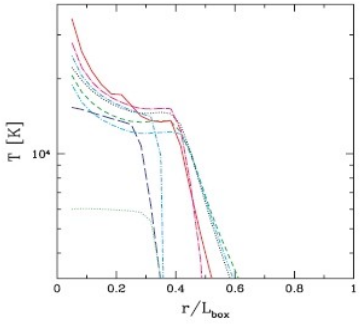

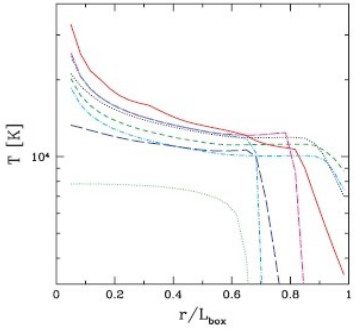

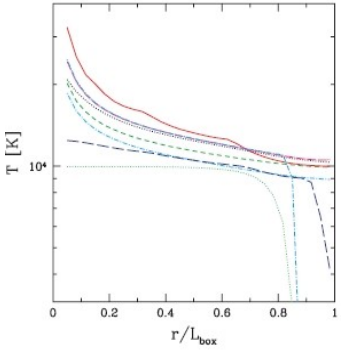

Test 5(grey): Classical HII expansion

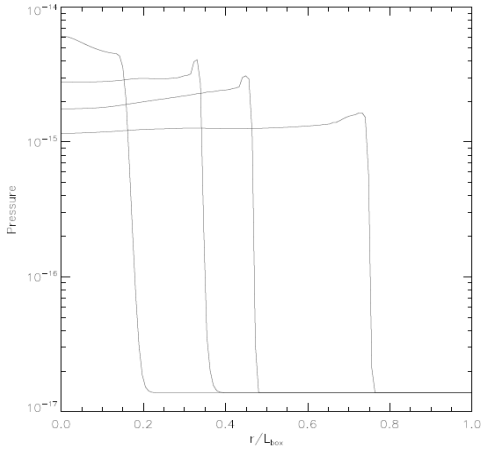

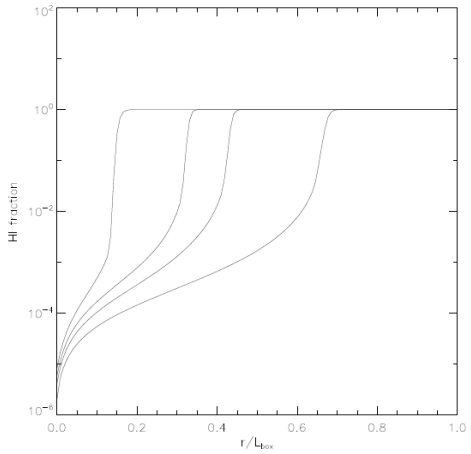

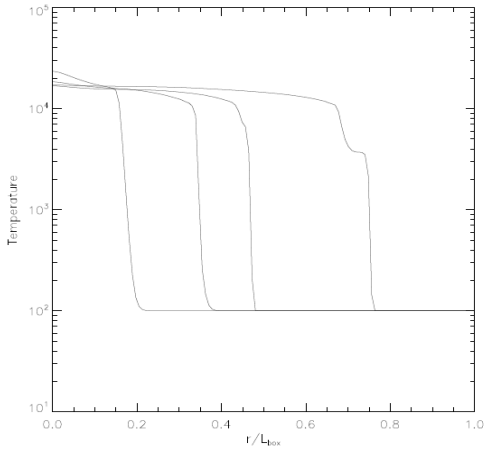

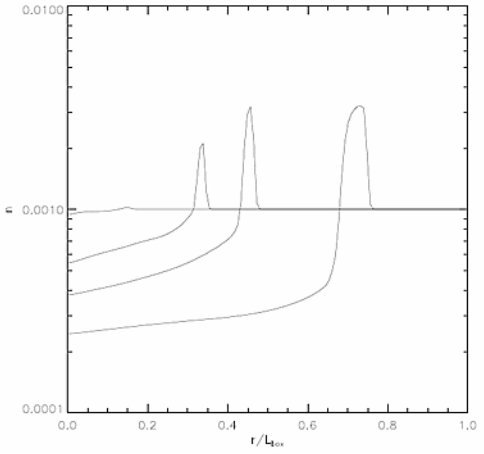

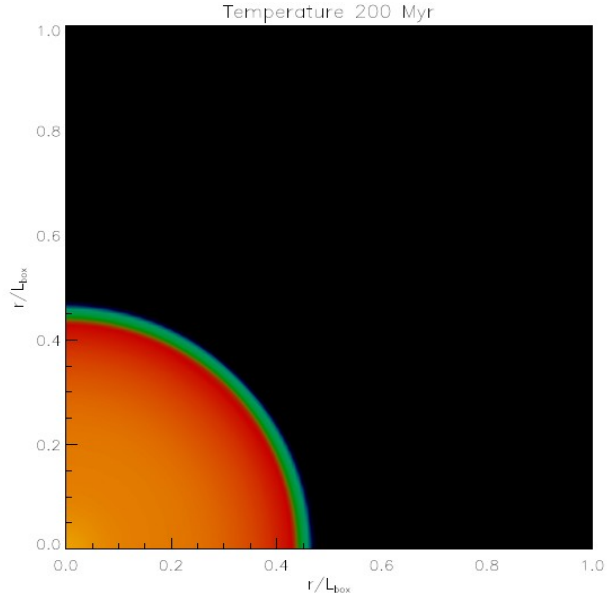

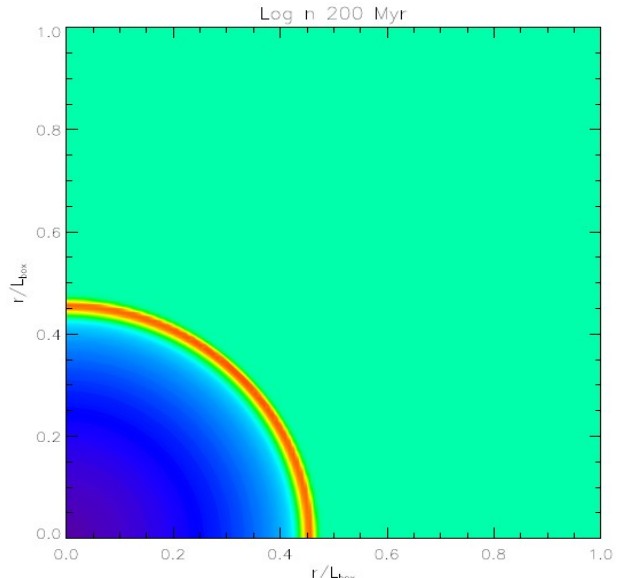

Profiles at t=10,100,200 and 500 Myrs

Cosmological I-fronts from Shapiro & Giroux (1987)

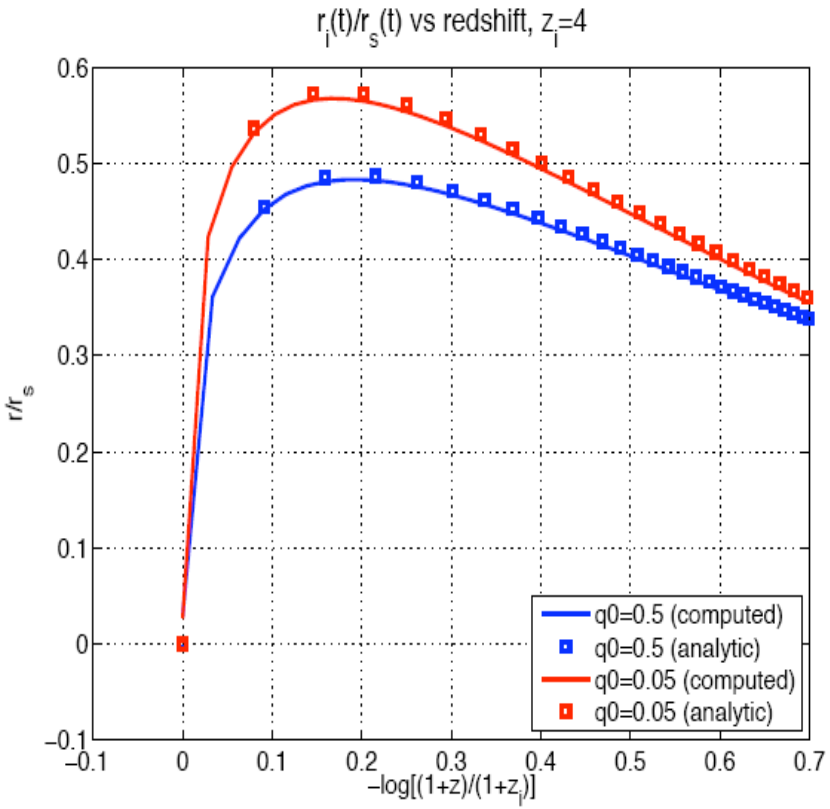

z_i : quasar redshift

$$r_I(t) = r_{S,i}\left(\lambda\, e^{-\tau(t)} \int_1^{a(t)} e^{\tau(\tilde{a})}\left[1 - 2q_0 + 2q_0(1+z_i)/\tilde{a}\right]^{-1/2} \mathrm{d}\tilde{a}\right)^{1/3}$$

$$\tau(a) = \lambda\, \left[6\, q_0^2\, (1+z_i)^2\right]^{-1} \left[F(a) - F(1)\right],$$

$$F(a) = \left[2 - 4q_0 - 2q_0(1+z_i)/a\right]\left[1 - 2q_0 + 2q_0(1+z_i)/a\right]^{1/2}$$

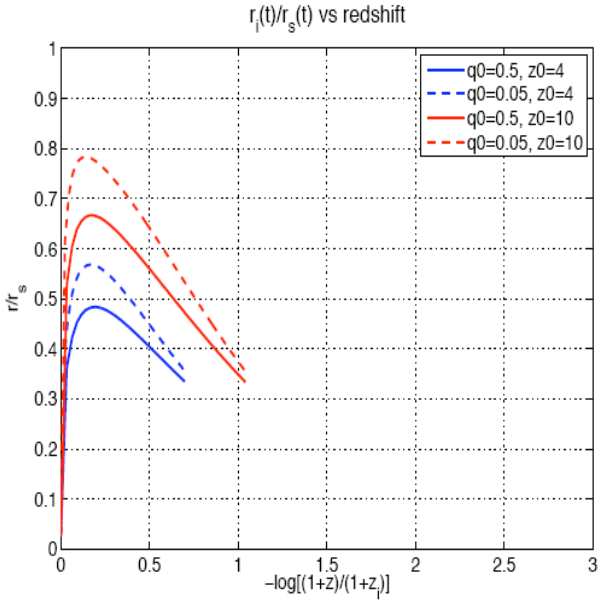

Parallel Scalability (SG problem)

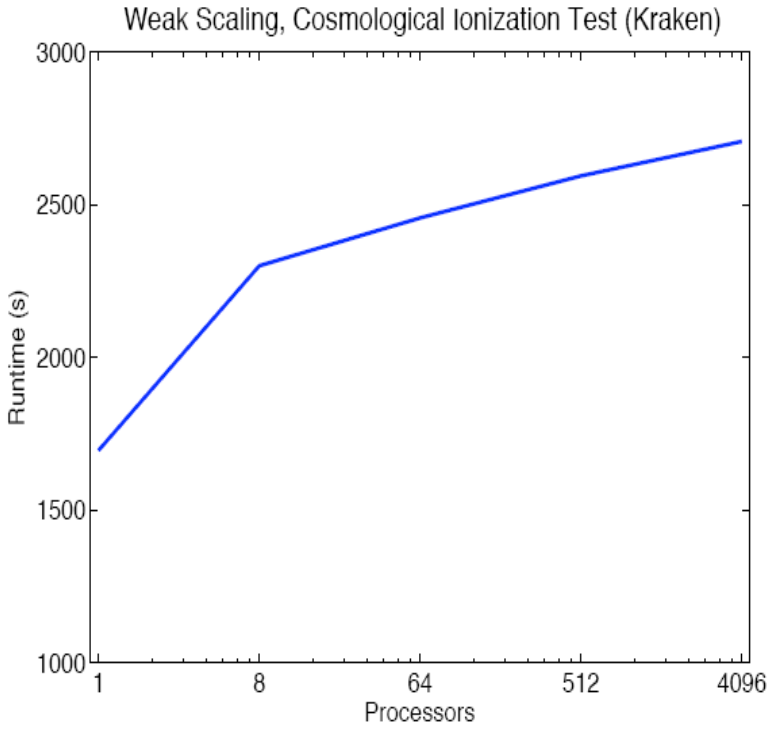

CPU scaling test performed on SG (q_0=0.5) problem between z=4 to z=3.

Initial spatial grid of 64^3 is increased by factors of 2^3. Number of processors is subsequently increased by the same factor.

Mesh	Processors	Time Steps	Run Time	Newton Its	CG Its	MG V-cycles
64^3	1	266	1694.38	322	914	2991
128^3	8	265	2299.60	274	799	2575
256^3	64	265	2456.58	268	787	2524
512^3	512	264	2594.50	265	780	2510
1024^3	4096	264	2707.30	265	780	2510

Current Work towards real-universe applications

- *Incorporate effective frequencies method: Obtain solutions at the three primary species ionization energies and interpolate between them and the optically thin background to reconstruct a "realistic" absorption spectrum*
- *Extension of the FLD solver to AMR hierarchy: requires HYPRE modification*
- *Point emissivity array nested in the AMR hierarchy at locations of star-formation or mass halo peaks for QSO driven photoionization*

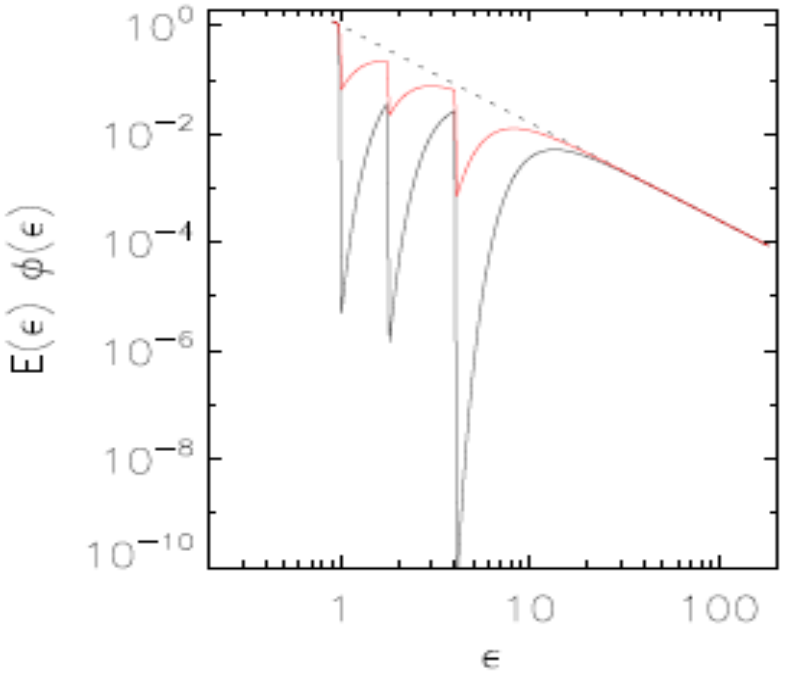

$$E_\epsilon = E_\epsilon^{OT} \times (E_1/E_1^{OT})^{S_1(\epsilon)} \times (E_2/E_2^{OT})^{S_2(\epsilon)} \times (E_3/E_3^{OT})^{S_3(\epsilon)}$$

Conclusions

We've achieved a second-order accurate (space and time) coupled solver for cosmological radiation, hydrodynamics, self-gravity and chemical ionization.

- Captures shock fronts in hydrodynamic fields, due to trusted PPM hydrodynamics approach.
- Efficient implementation due to semi-structured regular grids.
- Accurately solves couplings between radiation, ionization and gas energy, due to implicit formulation and Schur-complement linear solver.
- Achieves ultra-scalability, with current tests up to > 4000 processors, due to inner reliance on optimal multigrid methods.

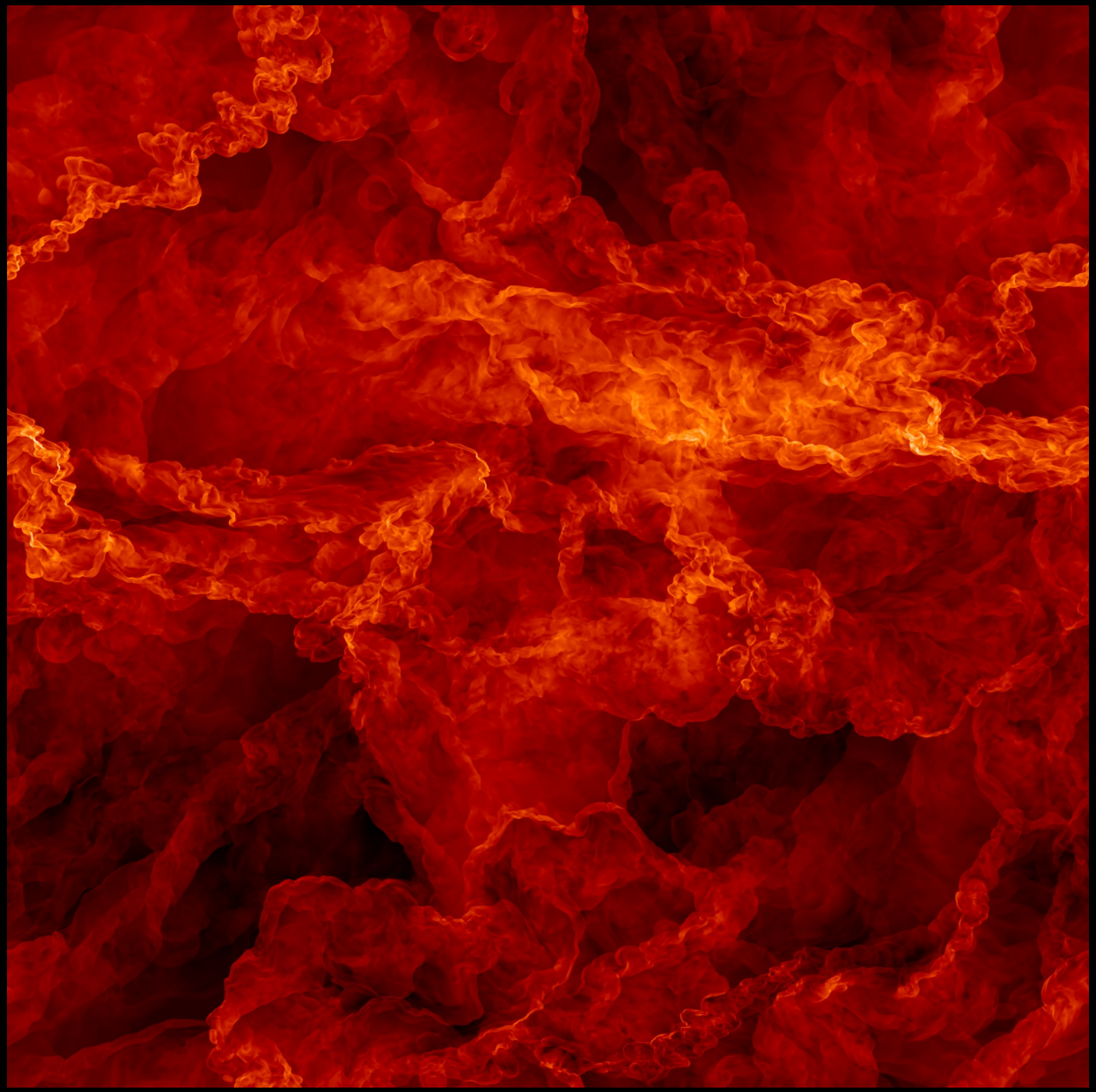

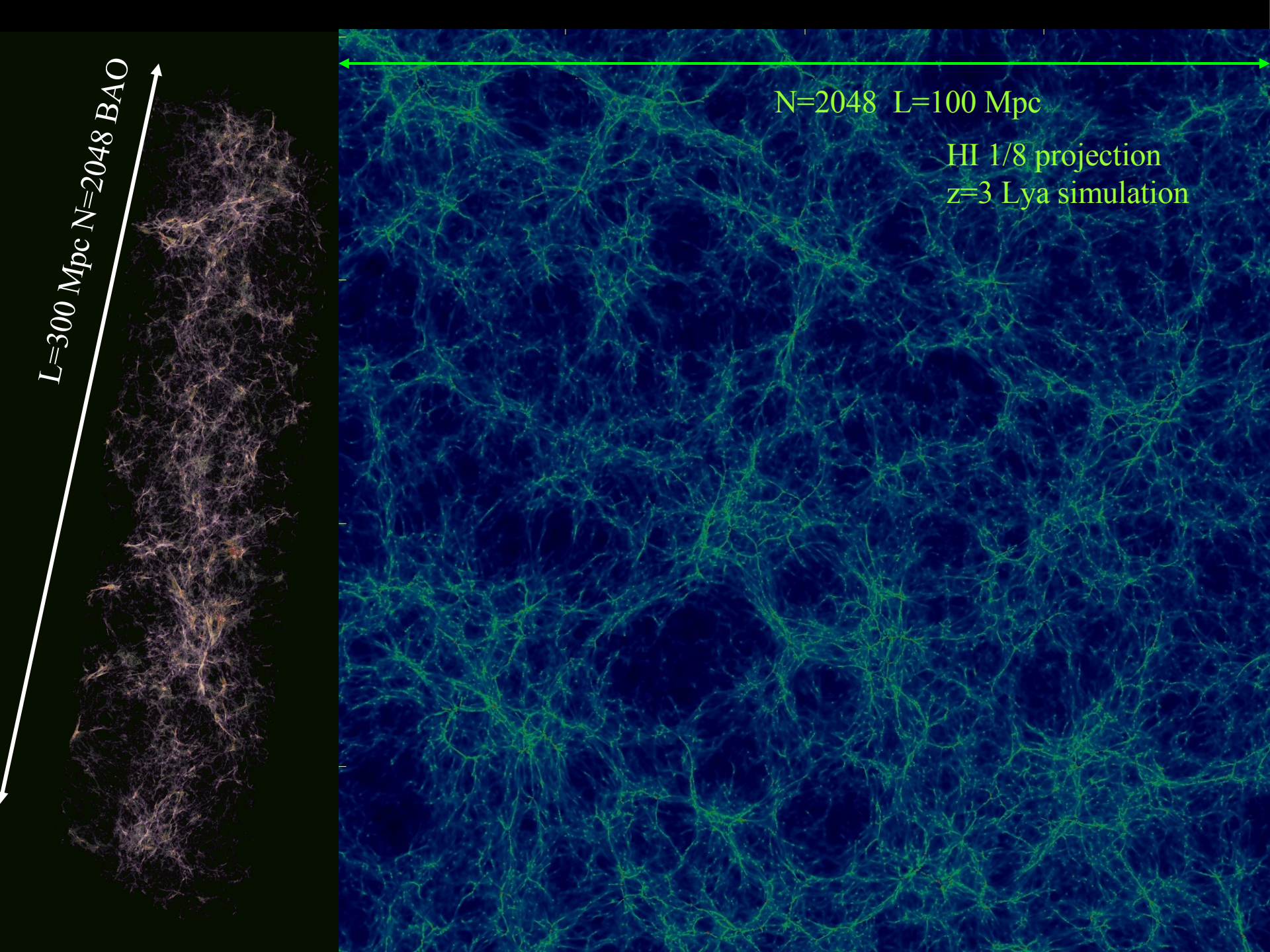
L=300 Mpc N=2048 BAO
N=2048 L=100 Mpc
HI 1/8 projection
z=3 Lya simulation